Biomechanical Study of the Thai Humerus with Humeral Shaft Fracture at Ninety Degrees Abduction

Panya Aroonjarattham[1], Kriskrai Sitthiseripratip[2,*], Banchong Mahaisavariya[3] and Kitti Aroonjarattham[4]

[1] Department of Mechanical Engineering, Faculty of Engineering, Mahidol University, Nakornpathom, Thailand, 73170
[2] National Metal and Materials Technology Center, Pathumthani, Thailand, 12120
[3] Department of Orthopaedics, Faculty of Medicine, Siriraj Hospital, Mahidol University, Bangkok, Thailand, 10700
[4] Department of Orthopaedics, Faculty of Medicine, Burapha University, Chonburi, Thailand, 20130
* Corresponding Author: E-mail: kriskrs@mtec.or.th, Phone: 0-2564-6500 Ext. 4021, 4022, 4378, Fax: 0-2564-6373

Abstract

The rotator cuff and deltoid muscles are the active muscle group when the humeri lift to abduction status. They are the main effect of the stress distribution on the implants and strain distribution on the humeral bone when the humeral shaft fractures occur. To stabilize the humeral shaft fracture, the standard humeral nail was used to fix the fracture gap with the antegrade insertion technique.

This study aims to find the effect on the implants and four fracture gaps along the humeral shaft at ninety degree abduction by finite element analysis with six muscular forces from the mechanical testing device which was validated the data. The result were shown that the fourth gap condition occur the highest strain on the fracture gap and the highest stress on the implant. The retrograde insertion technique must be proving for compare the appropriate technique for stabilize the humeral shaft fracture.

Keywords*:* Thai humerus, Humeral shaft fracture, Biomechanical study.

1. Introduction

For decades, nails fixation have been the most frequently used stabilizers for the surgical treatment for diaphyseal and metaphyseal fractures. They have been greatly improved in recent years and their indications have been widely extended [1]. Many computational works, based on finite element analysis, have been made to determine the stress distribution on implants [2-7] and bone [8-10], and to determine the structure of bone healing [11-15].

This study develops a three-dimensional finite element model of the humerus that consists of line action of rotator cuff and deltoid muscles to evaluate the stress distribution on standard humeral nail and strain on the Thai humeral bone with four gaps position.

2. Materials and Methods

To fully understand the reasons behind the greater biomechanical stability afforded by the standard humeral nail, a finite elements study was conducted. The finite element model was developed in which the geometry and position, bone material properties, nail geometry, nail location, gap positions, loading and boundary conditions were identical while the humerus position was abducted at ninety degree abduction, the gap position was occurred in shaft region [16] with first, second, third, and fourth gaps and nail location was varied to antegrade insertion. All finite element models were constructed by MSC PATRAN 2005 and all analyses were performed by MSC MARC/MENTAT 2005 finite element software packages.

2.1 Finite element model

The computer aided design (CAD) model of a three-dimensional humerus was the model of the average Thai humerus, which was created from the CT scans of 76 Thai cadaveric humeri. The humerus model consisted of cortex and cancellous layers. The set of internal fixation consisted of the standard humeral nail and the proximal and distal screws. The defect locations were evenly distributed along the humerus axis. Fractures were represented by 5 mm gaps [17-18] in the shaft region, as shown in Figure 1. Fractures in this region are considered unstable humeral shaft fractures.

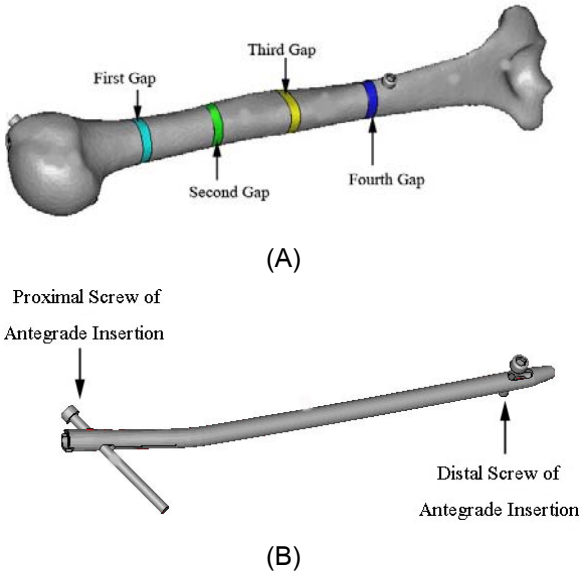

Fig. 1 The bone and implant models: (A) Humeral bone with four gap levels at the humeral shaft and (B) Implant models with antegrade insertion technique.

Four-node tetrahedral elements were used to build up the mesh of humeral bone and the standard humeral nail with proximal and distal screws in antegrade was shown in Figure 2. In the proximal and distal screw holes on the humeral nail, smaller elements (0.6-mm) were used to investigate the stress distribution and the displacement of the implant. The humerus–implant model had a total of 48,624 nodes and 192,637 elements.

Fig. 2 Finite element model of the standard humeral nail, the antegrade insertion.

2.2 Material properties

Linear elastic, isotropic, and

homogeneous material properties were assigned to all materials involved in the model [4, 7]. Material properties of all models are shown in Table 1. The fracture gaps were replaced by connective tissue to simulate healing status.

Table. 1 Material property applied for the FEA Model [3].

Model	Modulus (MPa)	Poisson's ratio
Cortical Bone	14,000	0.3
Cancellous Bone	600	0.2
Connective Tissue	3	0.4
Stainless Steel	200,000	0.3

2.3 Boundary conditions

Muscle attachment data, force magnitudes and orientations were derived from the mechanical testing device. The weight of the lower extremity, 3 kg, was applied to the distal humerus. The glenohumeral part was made to touch the humeral head for abduction status and its displacement was fixed for all directions.

2.4 The finite element analysis

Computational simulation contact of the bone and the nail requires finite element software equipped to incrementally update nodal displacements under a load while checking for penetration between the contacting bodies. The MARC contact algorithm determines whether any two bodies are contacting each other, and repositions nodes on the contact surface based on local normal stresses. An iterative Newton-Raphson method was used to ensure convergence to an equilibrium state at each load step. Fourteen contact bodies were defined as deformable bodies. These were separated into nine parts that were cortical bones, two parts that were cancellous bone, and three parts that were implants. All cortical bone parts in contact in glue condition and were in contact to cancellous bone in glue condition too. The humeral nail was in contact to the cortical and cancellous bone in touch condition, but the proximal and distal screws were in contact in glue condition. The analyses were performed under the frictionless mode to simplify the contact phenomena.

The influence of contact conditions in the fracture zone can be classified into two stages: before bone formation and after bone formation. Fifth analyses were performed in this study and are shown in Table 2.

Table. 2 List of conditions and fracture zone in the analyses.

Cases	Insertion Technique	Angle of Abduction	Fracture Zone
1	Antegrade	NinetyDegree	Intact
2	Antegrade	NinetyDegree	First Gap
3	Antegrade	NinetyDegree	Second Gap
4	Antegrade	NinetyDegree	Third Gap
5	Antegrade	NinetyDegree	Fourth Gap

3. Result

The maximum von Mises stress on the implant such as standard humeral nail, proximal screw, and distal screw illustrated nearly in mid-shaft site. All implants were strongly enough for use to fix the humeral shaft fracture in antegrade insertion technique. The maximum von Mises stress on the implant was shown in table 3 and the maximum strain on the fracture gaps were

shown in table 4.

Table. 3 The maximum von Mises stress on the implant with the antegrade insertion technique.

Ninety Degree Abduction	Gap position	Stress (Mpa)
Nail	Fourth Gap	296.60
Proximal Screw	Fourth Gap	33.40
Distal Screw	Fourth Gap	38.50

Table. 4 The maximum strain on the facture gap with the antegrade insertion technique.

Ninety Degree Abduction	Strain (microstrain)
First Gap	4,175-88,641
Second Gap	4,593-70,497
Third Gap	11,967-55,205
Fourth Gap	68,398-126,802

This status is a severe condition for normal abduction. Study of the total strain on the gaps showed that the fourth gap had the highest total strain with the antegrade insertion. The maximum strain was at the fourth gap and was between 68,398-126,802 microstrain, as shown in Figure 3.

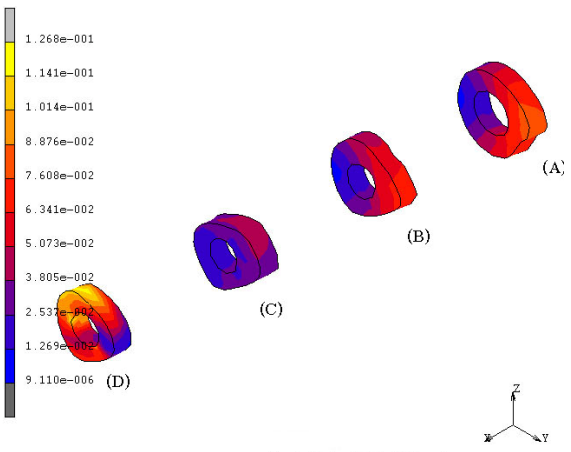

Fig. 3 The total strain on the three gaps with antegrade insertion and ninety degrees abduction: (A) First gap, (B) Seond gap, (C) Third Gap, and (D) Fourth gap.

4. Discussion

The muscle load configuration was applied for biomechanical study of a humeral shaft fracture with standard humeral nail fixation. The results will be discussed for the nail and the bone, respectively.

4.1 The standard humeral nail

Normally, the humeral nail had shared load from the bone but in case of ninety degree abduction is a severe condition that the bone was received the maximum load. The results were shown that the maximum stress on the implant occurred at the fourth gap fracture. All implant are strongly enough to fix the humeral bone fracture.

4.2 Humeral bone

The maximum strain arose on the fourth gap at ninety degrees abduction. The cause was the muscular force moment. The fourth gap had the maximum distance from the six muscular forces that act around the center of humeral head, and when the forces had a constant value, the moments vary with the distance. The strain distribution on the bone is the main factor affecting bone remodeling.

All gaps in cases of ninety degree abduction had strain greater than the pathological overload zone. The distance from all muscular forces to the fourth gap was higher than the distances to the other gaps, and this directly affected the moment that occurred. In the case of a humeral shaft fracture, the patient

did not lift the humeral bone to ninety degrees abduction

5. Conclusion

In this study, the muscular force of rotator cuff and deltoid created the initial load to the humeral bone for hang the weight of arm. It differ from the femur and tibia that the body weight was the main effect for create the initial load to act on the proximal bone. For the humeral shaft fracture, the patient will hang the arm in zero degree abduction to reduce the weight of arm for a good clinical result and retrograde insertion technique must be prove for compare this technique.

6. Acknowledgement

The authors would like to acknowledge the Department of Anatomy, Faculty of Medicine Siriraj Hospital, Mahidol University for their kindness support of the cadaveric humeral bone specimens, the National Metal and Materials Technology Center (MTEC), Thailand for their kindness support of the use of facilities.

7. References

[1] Hass N., Schutz M., Sudkamp N., and Hoffmann R., The new undreamed AO nails for the tibia and the femur, *Acta Orthopaedisca Belgica* (1995): 204-206.

[2] J. Grasa M.A., Perez J.A., Bea J.M., and Gracia-Aznar M.D., A probabilistic damage model for acrylic cement. Application to the life prediction of cemented hip implants, *International J. Fatigue* (2005): 1-14.

[3] Perez A., Mahar A., Negus C., Newton P., and Impelluso T., A computational evaluation of the effect of intramedullary nail material properties on the stabilization of simulated femoral shaft fractures, *J. Med Eng Phy* (2007): 1-6.

[4] Duda N.G., Mandruzzato F., Heller M., Goldhahn J., Moser R., Hehli M., Claes L., and Hass P.N., Mechanical boundary conditions of fracture healing: borderline indications in the treatment of undreamed tibial nailing, *J. Biomech* (2001): 639-650.

[5] Gupta S., Van der Helm F.C.T., and van Keulen F., The possibilities of uncemented glenoid component-a finite element study, *J.Clinbiomech* (2004): 292-302.

[6] Gupta S., Van der Helm F.C.T., and van Keulen F., Stress analysis of cemented glenoid prostheses in total shoulder arthroplasty, *J. Biomech* (2004): 1-10.

[7] Sitthiseripratip K., van Oosterwyck H., Sloten J.V., Mahaisavariya B., Bohez E.L.J., Suwanprateeb J., van Audekercke R., and Oris P., Finite element study of trochanteric gamma nail for trochanteric fracture, *J. Med Eng Phy* (2002): 99-106.

[8] Buchler P., Ramaniraka N.A., Rakotomanana L.R., Iannotti J.P., and Farron A., A finite element model of the shoulder: application to the comparison of normal and osteoarthritic joints, *J. Clinbiomech* (2002): 630-639.

[9] Plausinis D., Greaves C., Regan W.D., and Oxland T.R., Ipsilateral shoulder and elbow replacements: on the risk of periprosthetic fracture, *J. Clinbiomech* (2005): 1055-1063.

[10] Bitsakos C., Kerner J., Fisher I., and Amis A.A., The effect of muscle loading on the

simulation of bone remodeling in the proximal femur, *J. Biomech* (2004): 1-7.

[11] Gardner T.N., Stoll T., Marks L., Mishra S., and Tate M.K., The influence of mechanical stimulus on the pattern of tissue differentiation in a long bone fracture-and FEM study, *J. Biomech* (1999): 415-425.

[12] Epari D.R., Taylor W.R., Heller M.O., and Duda G.N., Mechanical conditions in the initial phase of bone healing, *J. Clinbiomech* (2006): 646-655.

[13] Gardner T.N., and Mishra S., The biomechanical environment of a bone fracture and its influence upon the morphology of healing, *J. Med Eng Phy* (2003): 455-464.

[14] Claes L.E., and Heigele C.A., Magnitudes of local stress and strain along bony surfaces prsdict the course and type of fracture healing, *J. Biomech* (1998): 255-266.

[15] Gemez-Benito M.J., Garcia-Aznar J.M., Kuiper J.H., and Doblare M., Influence of fracture gap size on the pattern of long bone healing: a computational study, *J. Theo Bio* (2005): 105-119.

[16] Verbruggen, J.P.A.M. and J.W.J.L. Stapert., Failure of reamed nailing in humeral non-union: an analysis of 26 patients, *J. Care Injuried* (2005): 430-438.

[17] Maldonado Z.M., Seebeck J., Heller M.O.W., Brandt D., Hepp P., Lill H., and Duda G.N., Straining of the intact and fractured proximal humerus under physiological-like loading, *J. Biomech* (2003): 1865-1873.

[18] Lin J., Inoue N., Valdevit A., Hang Y.S., Hou S.M., and Chao E.Y.S., Biomechanical comparison of antegrade and retrograde nailing of humeral shaft fracture, *J. Clinorthop* (1997): 203-213.

[19] Su C.S., Skedros G.J., Bachus N.K., and Bloebaum D.R., Loading conditions and cortical bone construction of an artiodactyls calcaneus, *J. Exp Bio* (1999): 3239-3254.